Molecularly imprinted polymer-based SAW sensor for label-free detection of cerebral dopamine neurotrophic factor protein

Kidakova, Anna

2020-04-01

Kidakova , A , Borozniak , R , Reut , J , Öpik , A , Saarma , M & Syritski , V 2020 , ' Molecularly imprinted polymer-based SAW sensor for label-free detection of cerebral dopamine neurotrophic factor protein ' , Sensors and Actuators B: Chemical , vol. 308 , 127708 . https://doi.org/10.1016/j.snb.2020.127708

http://hdl.handle.net/10138/342257
https://doi.org/10.1016/j.snb.2020.127708

Molecularly imprinted polymer-based SAW sensor for label-free detection of cerebral dopamine neurotrophic factor protein

Anna Kidakova[1], Roman Borozznjak[1], Jekaterina Reut[1], Andres Öpik[1], Mart Saarma[2] and Vitali Syritski[1]*

[1]Department of Materials and Environmental Technology, Tallinn University of Technology, Ehitajate tee 5, 19086 Tallinn, Estonia, vitali.syritski@taltech.ee

[2]Institute of Biotechnology, HiLIFE, University of Helsinki, P.O.Box 56, Viikinkaari 5D, FI-00014, Finland

Abstract

In this study we report for the first time on a surface acoustic wave (SAW) sensor modified with a molecularly imprinted polymer (MIP) selectively recognizing the cerebral dopamine neurotrophic factor (CDNF) protein. CDNF-MIP as a synthetic recognition element was prepared by a simple electrochemical surface imprinting approach allowing its reliable interfacing with SAW sensor. The optimal thickness of the MIP layer as well as a suitable pretreatment method were adjusted in order to improve the recognition capacity and selectivity of the resulting CDNF-MIP sensor. The selectivity of the sensor was studied by the carefully designed competitive binding experiments, which revealed that the sensor can sense CNDF confidently in label-free manner starting from 0.1 pg/ml. We anticipate that the findings can be a premise for fabrication of cost-effective research or diagnostics tools in the field of neurodegenerative diseases.

Abbreviations

CDNF, cerebral dopamine neurotrophic factor; CDNF-MIP, polymer film with molecular imprints of CDNF; HSA, human serum albumin; IgG, Immunoglobulin G; MANF, mesencephalic astrocyte-derived neurotrophic; mCD48, mouse recombinant cluster of differentiation 48; MIP, molecularly Imprinted polymer; NIP, non-imprinted polymer; NTF, neurotrophic factor; PBS, phosphate buffer saline; SAW, surface acoustic wave sensor;

1. Introduction

In clinical diagnostics, the research in the discovery and detection of biomarkers of human diseases, neurological and mental disorders has become of great demand due to the increase in the prevalence of these diseases over the last decades and the urgent need for their early stage diagnosis [1]. For example, neurotrophic factor (NTFs) proteins are a family of proteins secreted from neurons and glial cells, and supporting the survival of neurons [2]. NTFs were found to be associated with a number of neurological diseases (NDs) such as Alzheimer's, Parkinson's and mental disorders and have been tested in clinical trials of several neurodegenerative diseases [3–6].

Cerebral dopamine neurotrophic factor (CDNF), and mesencephalic astrocyte derived neurotrophic factor (MANF) form a new family of unconventional NTFs that have been shown to be promising candidates for the treatment of Alzheimer's and Parkinson's [6–9]. In animal models of Parkinson's disease these NTFs can support the survival of neurons and regenerated neuronal axons opening a possibility for the development of disease modifying treatments. CDNF is currently tested in phase I-II clinical study on Parkinson's disease patients in three Scandinavian medical centres [10]. The abnormal levels of NTFs in the blood may be associated with a number of NDs [11], mental disorders [3] and diabetes [12]. Serum and/or cerebrospinal fluid (CSF) concentration of a specific NTF could therefore be a potential biomarker for early-stage diagnosis and/or the follow-up of neuroprotective therapies.

Today, ELISA is one of the most commonly used immunological assays, applicable in both research and diagnostics, providing a quantitative detection of specific proteins, including NTFs, in serum samples [13]. In spite of its high specificity and low limit of detection (LOD) [14], ELISA suffers from several disadvantages such as laborious, lengthy procedure, the use expensive bioassay kits, low reliability and reproducibility in serum samples because of the cross-reaction with other antibodies.

To address these issues valuable alternatives to the traditional detection methods e.g. based on label-free sensor platform have been intensively studied [15]. The sensors based on the acoustic wave transduction mechanism seem to be a prospective for diagnostics purposes since they combine direct detection, simplicity in handling, real-time monitoring, and good sensitivity with a more reduced cost. Thus, Surface Acoustic Wave sensors (SAW) being fully compatible with large-scale fabrication and multiplexing technologies may provide substantial advantages in biosensing where electron transfer processes are hindered [16]. However, the reported label-free biosensing systems mostly utilize labile biological recognition elements (e.g. enzymes, DNA, antibodies) [17,18]. Moreover, applications for label-free sensing of NTF-proteins are very scarce [19,20].

Coupling label-free sensor platforms with synthetic recognition elements that avoid the disadvantages associated with the use of biological receptors in order to provide a reproducible and fast analysis of a biological sample, is of great importance. Molecular imprinting is one of the state-of-the-art techniques to generate robust synthetic molecular recognition materials with antibody-like ability to bind and discriminate between molecules [21]. The technique can be defined as the process of template-induced formation of specific molecular recognition sites in a polymer matrix material. The main benefits of these polymers, so-called Molecularly Imprinted Polymers (MIPs), are related to their synthetic nature, i.e., excellent chemical and thermal stability associated with reproducible, cost-effective fabrication. MIP receptors have been shown to be a promising alternative to natural biological receptors in biosensors providing more stable and low-cost recognition

elements [22,23].

It should be noted that robust interfacing of a MIP with a sensor platform capable of responding upon interaction between the MIP and a binding analyte is a key aspect in the design of a MIP-based sensor. Recently, the use of an electrosynthesis approach for the facile integration of MIPs with label-free sensor platforms was reported [24–27].

The application of MIP-based sensors for diagnostics has been extensively studied. Thus, the detection of cancer biomarkers - prostate specific antigen [28], epithelial ovarian cancer antigen-125 [29], carcinoembryonic antigen [30], cardiovascular disease biomarkers - myoglobin [31] and cardiac troponin T [32] by MIP-modified sensors have been reported. In addition, MIP receptors for selective extraction of Alzheimer's disease biomarker, β-amyloid peptides, has been studied by Sellergren's group [33]. As concerns the imprinting of NTFs, so far only the selective recognition of another growth factor family protein - vascular endothelial growth factor (VEGF-A) by hybrid MIP nanoparticles as well as by MIP thin layer on SPR and screen-printed electrodes (SPE) has been reported [34–36]. Very recently, our group demonstrated the preparation of a photopolymerized MIP film integrated to a SPE and capable of selective recognition of brain-derived neurotrophic factor [37].

In this study, we report for the first time on the fabrication of MIP-based SAW sensor for label-free detection of CDNF. In this sensor, CDNF-MIP prepared by a surface imprinting approach, was utilized as a synthetic recognition element firmly interfaced with SAW sensing surface in the course of a simple electrochemical synthesis. As compared to electrochemical detection, we reported previously, the use of a mass-sensitive transducer such as SAW benefits from the absence of necessity to employ a redox pair as an electrochemical indicator as well as for ensuring the sufficient electrical conductivity at the electrode/solution interface for reliable and fast sensing of CDNF.

2. Experimental

2.1 Chemical and materials

Sodium chloride (NaCl), 4-aminothiophenol (4-ATP), 2-mercaptoethanol, m-phenylenediamine (mPD), dimethyl sulfoxide (DMSO), human serum albumin (HSA), and sodium dodecyl sulfate (SDS) were purchased from Sigma-Aldrich. Human recombinant Cerebral Dopamine Neurotrophic Factor (CDNF, 18.5 kDa, calculated pI 7.68), human recombinant mesencephalic astrocyte-derived neurotrophic factor (MANF, 18.1 kDa, calculated pI 8.55), and mouse recombinant mCD48 (cluster of differentiation 48, 22.2 kDa, pI 9.36) were provided by Icosagen AS (Tartu, Estonia). 3,3'-dithiobis [sulfosuccinimidylpropionate] (DTSSP) was purchased from Thermo Fisher Scientific Inc. Glycerol, sulfuric acid, hydrogen peroxide, and ammonium hydroxide were purchased from Lach-ner, S.R.O. All chemicals were of analytical grade or higher and were used as received without any further purification. Ultrapure Milli-Q water (resistivity 18.2 MΩ·cm at 25°C,

EMD Millipore) was used for the preparation of all aqueous solutions. Phosphate buffered saline (PBS) solution (0.01 M, pH 7.4) was used to prepare synthesis and analyte solutions.

2.2 Preparation of CDNF-MIP sensor

The technological basis for a CDNF-MIP sensor was a label-free SAW system (SamX, NanoTemper Technologies GmbH, München, Germany). SAW system uses a pair of Love-wave sensor chips manufactured from ST-cut quartz substrates. Every sensor chip has four sensor elements (sensing surface 5x1.2 mm per sensor element). The shear-horizontal acoustic waves in the elements are generated by radio-frequency (RF) signal (between 147 and 150 MHz) applied to the input interdigital transducers (IDTs). The waves concentrated within the gold-coated SiO_2 guiding layer are converted back to an RF signal upon arriving to the output IDTs. The phase shift of RF signals measured by a Vector Network Analyzer is proportional to the mass loading on a sensing surface of the chip. The sensing surface of the sensor chips was modified with CDNF-MIP as a synthetic recognition layer using an electrochemical surface imprinting approach. The protocol for synthesis of CDNF-MIP was adapted from our previous work [26] (Fig. 1). Thus, firstly the sensor surface was modified with the target protein (CDNF) immobilized via 4-ATP/DTSSP linker system having the cleavable S-S bond, followed by electropolymerization of mPD conducted at the constant potential (0.6 V versus Ag/AgCl/1M KCl) applied to the sensor surface until defined amount of electrical charge had been passed.

Poly(m-phenylenediamine) (PmPD) film thicknesses were determined by a spectroscopic ellipsometer (SE 850 DUV, Sentech Instruments GmbH, Berlin, Germany). Ellipsometric parameters ψ and Δ were measured from three spots for each sample in ambient air confining the wavelength range between 380 and 850 nm at the angle of incidence of 70°. The spectra were fitted (SpectraRay 3 software) with the optical model containing a one-layer Cauchy layer on the top of the gold and the thicknesses were determined.

To form the molecular imprints the polymer was treated in 0.1 M ethanolic solution of 2-mercaptoethanol to cleave the S-S bond in the linker system and, subsequently, in the aqueous solution of 3 M NaCl and DMSO. The respective reference films i.e those that do not have the molecular imprints of CDNF in the polymer, non-imprinted polymers (NIPs), were prepared by very similar way as CDNF-MIP, but excluding the treatment in mercaptoethanol. Thus, the template proteins are still covalently retained in the NIP matrix hindering the possibility to rebind CDNF at this location.

2.3 Rebinding and selectivity studies

The sensor chips, modified with CDNF-MIP and the respective reference, NIP layers (Fig. S1), were loaded into SAW system and equilibrated with the degassed running buffer solution (PBS, pH 7.4) at a flow rate of 25 µl/min until a stable baseline was established. The temperature of the running solutions and the chips was controlled with Peltier element with +/-0.01 °C precision and kept constant at 22°C. Then the consecutive injections of the

analyte solutions in order from lower to higher concentrations were applied (from 50 ng/ml to 33.75 µg/ml of CDNF on PBS buffer) and the phase-shift responses versus time (sensorgrams) were recorded. The details of kinetics analysis of the sensorgrams are given in section S1 of SI. The selectivity of the CDNF-MIP sensor was studied with the help of a kinetic titration series, where the solution of either CDNF or an interfering homologous protein MANF in order from a low to a high concentration (from 5 ng/ml to 300 ng/ml) were sequentially injected onto the sensor elements. The respective solution were prepared in PBS buffer and contained the constant concentration of mCD48 (1.25 µg/ml). The selectivity was assessed by comparison of the residual responses at infinite dissociation which appeared after washing the sensor surface with running PBS buffer solution for 25 min (see section S2). In the competitive binding assays [38,39], the various concentrations (from 10^{-6} to 10^{-2} ng/ml) of either CDNF or MANF (competitor) were allowed to compete in PBS buffer with the constant amount of IgG (500 ng/ml) for the binding sites in CDNF-MIP. Additionally, the samples having different ratios of CDNF to MANF (10^{-2}:10^{-3} ng/ml or 10^{-3}:10^{-2} ng/ml) and IgG (500 ng/ml) were applied to assess the ability of the sensor to discriminate between CDNF and MANF (see section S2).

3. Results and discussion

3.1 Optimization of CDNF-MIP sensor preparation

The molecular imprinting strategy used in this study employs the bottom-up approach [26] in order to generate the macromolecular imprints resided on at/close to the surface of the polymeric film. Thus, for such MIP, the deposition of a polymer with an appropriate thickness is one of the most crucial tasks in order to avoid irreversible entrapment of a macromolecular template and infeasibility of its removal during the subsequent washing out procedures. The effect of polymer thickness on the performance of the resulting macromolecular-MIP has been already demonstrated in our previous study [26]. Thereby, we began to design CDNF-MIP paying special attention to the careful choice of an optimal thickness of the polymer matrix. In order to choose the range of the appropriate thicknesses for the polymer film, which confines, but does not irreversible entrap CDNF, the length of the whole structure containing the linker system and CDNF, was theoretically estimated (Fig. 2). Assuming that covalent attachment of CDNF via the succinimidyl group of DTSSP proceeds predominantly through its lysine residues that are abundant in the protein, the size of the resulting structure with random orientations of CDNF might vary from ca. 5.1 to 7.5 nm. Thus, polymer films confining the immobilized CDNFs till the middle of their possible front dimensions i.e. films with thicknesses between approx. 3.4 and 4.6 nm would be a good starting point in finding an optimal one for CDNF-MIP.

The correlation between the amount of electrical charge applied during the *in-situ* electrodeposition of the polymer and the thicknesses of the resulting CDNF-MIP films is presented in Fig. 2. As it can be seen, the thicknesses for CDNF-MIP varied linearly

(R^2=0.998) across the applied electric charge range. This makes prediction of the thickness in the range of ca. 3 nm to 8 nm quite certain in a convenient way by controlling the applied charge. The optimal thickness was elucidated after calculation of the molecular imprinting effect or the imprinting factor (*IF*) for every pair of CDNF-MIP and NIP characterized by the same thicknesses:

$$IF = Q_{eq(MIP)}/Q_{eq(NIP)} \quad (1)$$

where $Q_{eq(MIP)}$ and $Q_{eq(NIP)}$ are phase-shift responses at the equilibrium upon injection of a particular concentration of CDNF onto CDNF-MIP- and NIP-modified sensor elements, respectively. Thus, among the CDNF-MIPs having thicknesses ranging between 0.5 and 9 nm, one with PmPD generated by 1 mC/cm^2 (ca. 2.3 nm) demonstrated the highest *IF* (1.2) (Fig. 3a). It should be noted that there was significant non-specific binding on NIPs resulting in marginal differences in responses between CDNF-MIP- and NIP-modified sensor elements. This makes values of IFs not prominent enough to justify confidently that 2.3 nm thick polymer would be an optimal one for CDNF-MIP. In order to reduce the non-specific binding, the CDNF-MIP and NIP films were underwent the treatment in 0.01 M PBS solution containing 0.04 mg/ml HSA beforehand the rebinding experiments.

Although the treatment with HSA significantly suppressed the response amplitudes, the noticeable difference between CDNF-MIP- and NIP-modified sensor elements was achieved (Fig. 3b). This also affected the ranking of the optimal polymer thicknesses. After the treatment in HSA, CDNF-MIPs with thickness of 4.4 nm (2 mC/cm^2) had the highest relative rebinding of CDNF as judged by IF equal to about 2 (Fig. 3b). The found optimal thickness correlates well with the concept of surface imprinting approach used in this study. At such thickness the polymer confines about the median dimension of CDNF, and, in turn, likely does not hinder its successful extraction to leave behind a selective molecular cavity. Thus, the use of electrochemical polymerization for protein-MIP is a very sophisticated method to generate precisely such ultrathin polymer matrices by just control the applied electrochemical charge.

3.2 Rebinding studies

The CDNF-MIP sensors were characterized in terms of their capability to rebind CDNF by monitoring and comparing its binding kinetics on CDNF-MIP and NIP surfaces. Since, according to the applied synthesis strategy, the template proteins were not removed from NIP, we considered the NIP as the CDNF-MIP with completely occupied specific binding sites and, analysing the obtained binding profiles, assumed that during the rebinding process (i) such a NIP surface exhibited only nonspecific protein adsorption and (ii) on the respective CDNF-MIP surface the nonspecific adsorption could occur to the same extent. Thus, in order to reference out the contribution of nonspecific interactions in the response signals, the binding profiles on the CDNF-MIP were corrected by subtracting the corresponding binding profiles observed on the NIP surfaces.

After the correction, the responses of the CDNF-MIP sensor demonstrated well pronounced analyte concentration-dependent binding profiles and allowed fitting them to the pseudo-first order kinetics model (Eq. S1) (Fig. S2). This model has been previously successfully applied for description of binding kinetics on MIPs [40]. In this study, the model still gave a decent fit to the experimental kinetics data with a coefficient of determination (R^2) in the range of 0.944-0.994 (Table S1) and allowed predicting the equilibrium responses (Q_{eq}) at every injected concentration of CDNF.

We examined two binding isotherm models to describe Q_{eq} vs concentration data: Langmuir (L) and Langmuir–Freundlich (LF) (Fig. 4). While L model assumes that a monolayer of adsorbate is formed on a homogeneous surface of the adsorbent [41], LF model, being a continuous distribution model, can be applied for modelling a more complex interaction between the molecule and the surface of the adsorbent with the participation of binding sites having different levels of affinity [42]. As expected, the LF model provided somewhat better agreement with the binding isotherm data than the L model (coefficient of correlation 0.990 and 0.975, respectively (Table S2)). As has been shown previously, most MIPs often behave as heterogeneous systems, and thus the LF model would be more universally applicable to their characterization, since it takes into account heterogeneity of binding sites and is able to model binding behavior in a wider concentration range up to saturation [42,43]. Additionally, the Scatchard plot i.e the experimental binding isotherm in the Q_{eq}/C vs. Q_{eq} format, clearly shows the heterogeneity of the binding sites (Fig. 4, insert). Two separate straight line parts on the curve of the isotherm indicate that there are sites with different affinities. The flat and steep lines describes the sites with low and high affinity, respectively [42].

The heterogeneity of the current CDNF-MIPs can be explained by the fact that CDNF imprints were formed by CDNFs randomly oriented towards the sensor surface. Indeed, to form the CDNF-MIP, CDNFs were initially immobilized on the surface through the covalent interaction of primary amines of the lysine side chain of CDNF with the active group of DTSSP. Since the primary amines are located over the entire surface of CDNF, it could be immobilized with different orientations to the surface leading to the formation of the imprinted sites with different binding energy in the course of the subsequent imprinting process.

3.3 Selectivity studies

Several binding assays were carried out in order to assess the feasibility and selectivity of detecting CDNF by CDNF-MIP sensor. In the first test, CDNF-MIP sensor was investigated in terms of its capability to rebind the target protein, CDNF with respect to a protein having a very similar structure [4], same size, but a slightly different pI such as MANF and can be thus, a suitable pair to assess the selectivity of the prepared CDNF-MIP layer. The test was carried out in the presence of mCD48 having pI value higher than CDNF and MANF in order

to cause an additional nonspecific background and thus somewhat simulate additional complexity in scenarios for the selectivity testing.

As it can be seen, although the sensor is responsive to every applied injection, the sharp rises appear only upon injection of the solutions containing CDNF (Fig. 5a). During the dissociation stages the responses do not returned back to the baseline, but are gradually shifted to higher values indicating that a part of protein molecules remained bound to the sensor surface. Taking into account such behavior, we analyzed the sensor responses by calculating the residual binding values at dissociation stage, Q_{res} (see Section S2 and Table S3 in SI for details) and compared these values between CDNF and MANF injection series in order to assess the capability of the sensor to distinguish the respective proteins (Fig. 5b). The noticeable increase of Q_{res} in favour of CDNF containing mixtures can be observed already after the first concentration applied (5 ng/ml) eventually reaching 4-fold difference after the final injection (300 ng/mL). A possible explanation for this phenomenon could be the higher affinity of the CDNF-MIP surface towards CDNF molecules that remain bound to CDNF-MIP at much higher extent than MANF molecules. Under the given assay conditions, the CDNF-MIP sensor shows a linear response to CDNF in the concentration range from 5 to 50 ng/ml, with limit of detection (LOD) and limit of quantitation (LOQ) of 4.2 ng/ml and 14 ng/ml (Fig. S3).

To further examine selectivity of the CDNF-MIP sensor, we designed a label-free binding assay, where various concentrations of either CDNF or MANF were allowed to compete with the constant amount of IgG for the binding sites in CDNF-MIP. Specifically, in the assay, we looked into the inhibition of non-specific binding of a relatively massive protein such as IgG on the surface of the CDNF-MIP caused by the increasing concentration of competing protein in the applied mixture.

The optimal concentration of IgG in the assay was selected by plotting the binding isotherm of non-specific adsorption of IgG on the surface of the CDNF-MIP. As it can be seen, adsorption of IgG is linear versus the concentration in the range of 31.25 to 1000 ng/ml, but tends to saturate afterwards (Fig. S4). Therefore, the concentration of 500 ng/ml IgG was selected for the following binding assays as one could provide a noticeable effect on the competitive replacement of IgG on the CDNF-MIP surface. The concentrations above 500 ng/ml might be redundant and can hinder observing the effect.

Although, little is known about the nature of protein recognition sites in MIPs, it was reasonable to expect that in the given competitive binding assays CDNF-MIP sensor was going to be more responsive to CDNF i.e. the mixtures containing CDNF and IgG would evoke stronger inhibitions of IgG binding than those containing MANF and IgG. As demonstrated by Fig. 6, indeed the normalized response, Q_n, decreased (about 75%) upon injection of the mixture containing 0.01 ng/ml CDNF, i.e. obviously, the heavier protein (IgG) is replaced with the lighter one (CDNF). Conducting the very same competitive assay

with MANF instead of CDNF, resulted in much less inhibition of the response (about 15%), that is, the replacement of IgG from the recognition sites is less efficient in this case. If both CDNF and MANF competed with IgG in the same solution then it was still clearly seen that the significant inhibition of the signal was induced namely by the presence of CDNF in the sample rather than the presence of MANF (Fig. S5).

The competitive binding assay data are fitted by three parameter dose response curves revealing IC50 values for CDNF and MANF assays with a marginal difference: 0.6 versus 0.9 pg/ml, respectively (see Section S2 and Table S4). Nevertheless, taking into account the high similarity in the three-dimensional structures of CDNF and MANF [44,45] and the fact that CDNF was identified to be homologous to MANF with 59% amino acid identity in human proteins [4], the given assay still supports clearly that CDNF-MIP surface preferentially binds CDNF than MANF. The limit of detection in this assay, calculated as the analyte concentration causing a 20% inhibition (IC_{20}), corresponded to 0.1 pg/ml. However, even 10 pg/ml concentration of MANF is unable to cause such significant inhibition to CDNF binding response. The found LOD is significantly below the CDNF concentrations found in human serum [46].

Conclusions

We have demonstrated the possibility of using a MIP-based synthetic receptor to build a SAW sensor capable of detecting a neurotrophic factor protein, CDNF, in label-free manner. The electrochemical surface imprinting approach enabled a simple and rapid preparation of the polymeric matrix possessing the selectivity to CDNF, i.e. CDNF-MIP, directly on the sensor surface. We found that the thickness of the polymer matrix is critical and should be precisely adjusted in order to achieve the notable imprinting effect in the resulting CDNF-MIPs. Polymers with thicknesses, confining about the median dimension of a macromolecule, thus likely provide its successful extraction and leaving behind a molecular cavity capable of efficient and selective rebinding. Moreover, intrinsic affinity of PmPD-based matrix to CDNF was needed to be suppressed in order to properly assess imprinting effect. Nevertheless, the presence of intrinsic affinity in the resulting CDNF-MIP would not likely necessarily disturb the sensor response, but could be considered for designing competitive assays, where the target protein displaces interfering one from the MIP-modified sensor surface. As demonstrated, the prepared CDNF-MIP sensor clearly differentiated between CDNF and its homologue - MANF even in the presence of IgG in the test solution showing a response at sub pg/ml range.

We anticipate that our results provide guidelines for synthesis of MIPs applicable for detection of other essential NFs. These NF-selective MIPs can work well as synthetic recognition layers with other label-free sensing platforms such as surface plasmon resonance and quartz crystal microbalance, where accumulated mass is measured at the surface of their transducers. Further study is needed to investigate the sensor capability

detecting CDNF in complex matrixes as body fluids. If this works the adaptation of our results to portable sensor platforms will pave the way for the much-needed cost-effective research or diagnostics tools in the field of neurodegenerative diseases. Efforts along those lines are currently in progress to validate detection of CDNF in body fluids of real patient samples that have been verified with CDNF and MANF ELISAs.

Acknowledgements

This work was supported by the Estonian Research Council grant (PRG307) and by the Jane and Aatos Erkko Foundation. The authors thank Dr. Andreas Furchner from Leibniz-Institut für Analytische Wissenschaften – ISAS – e. V. for the VIS ellipsometry measurements. The authors thank Icosagen AS and prof. Mart Ustav personally, for kindly providing the neurotrophic factor proteins.

References

[1] World Health Organization, Neurological Disorders: Public Health Challenges, World Health Organization, Geneva, Switzerland, 2006. http://whqlibdoc.who.int/publications/2006/9241563362_eng.pdf.
[2] Y.S. Levy, Y. Gilgun-Sherki, E. Melamed, D. Offen, Therapeutic potential of neurotrophic factors in neurodegenerative diseases, BioDrugs Clin. Immunother. Biopharm. Gene Ther. 19 (2005) 97–127.
[3] K. Hashimoto, Brain-derived neurotrophic factor as a biomarker for mood disorders: An historical overview and future directions, Psychiatry Clin. Neurosci. 64 (2010) 341–357. https://doi.org/10.1111/j.1440-1819.2010.02113.x.
[4] M. Lindahl, M. Saarma, P. Lindholm, Unconventional neurotrophic factors CDNF and MANF: Structure, physiological functions and therapeutic potential, Neurobiol. Dis. 97 (2017) 90–102. https://doi.org/10.1016/j.nbd.2016.07.009.
[5] M. Saarma, P. Lindholm, U. Arumäe, Neurotrophic Factors, Mov. Disord. (2012) 129–140.
[6] M.H. Voutilainen, U. Arumae, M. Airavaara, M. Saarma, Therapeutic potential of the endoplasmic reticulum located and secreted CDNF/MANF family of neurotrophic factors in Parkinson's disease, FEBS Lett. 589 (2015) 3739–48. https://doi.org/10.1016/j.febslet.2015.09.031.
[7] D. Lindholm, J. Mäkelä, V. Di Liberto, G. Mudò, N. Belluardo, O. Eriksson, M. Saarma, Current disease modifying approaches to treat Parkinson's disease, Cell. Mol. Life Sci. 73 (2016) 1365–1379. https://doi.org/10.1007/s00018-015-2101-1.
[8] P. Lindholm, M.H. Voutilainen, J. Lauren, J. Peranen, V.M. Leppanen, J.O. Andressoo, M. Lindahl, S. Janhunen, N. Kalkkinen, T. Timmusk, R.K. Tuominen, M. Saarma, Novel neurotrophic factor CDNF protects and rescues midbrain dopamine neurons in vivo, Nature. 448 (2007) 73–7. https://doi.org/10.1038/nature05957.
[9] Y.A. Sidorova, M. Saarma, Glial cell line-derived neurotrophic factor family ligands and their therapeutic potential, Mol. Biol. 50 (2016) 521–531. https://doi.org/10.1134/s0026893316040105.
[10] H.J. Huttunen, M. Saarma, CDNF Protein Therapy in Parkinson's Disease, Cell Transplant. (2019) 963689719840290. https://doi.org/10.1177/0963689719840290.
[11] M. Ventriglia, R. Zanardini, C. Bonomini, O. Zanetti, D. Volpe, P. Pasqualetti, M. Gennarelli, L. Bocchio-Chiavetto, Serum brain-derived neurotrophic factor levels in different neurological diseases, BioMed Res. Int. 2013 (2013) 901082. https://doi.org/10.1155/2013/901082.
[12] E. Galli, T. Härkönen, M.T. Sainio, M. Ustav, U. Toots, A. Urtti, M. Yliperttula, M. Lindahl, M. Knip, M. Saarma, P. Lindholm, Increased circulating concentrations of mesencephalic astrocyte-derived neurotrophic factor in children with type 1 diabetes, Sci. Rep. 6 (2016) 29058. https://doi.org/10.1038/srep29058.
[13] B. Elfving, P.H. Plougmann, G. Wegener, Detection of brain-derived neurotrophic

factor (BDNF) in rat blood and brain preparations using ELISA: pitfalls and solutions, J. Neurosci. Methods. 187 (2010) 73–7. https://doi.org/10.1016/j.jneumeth.2009.12.017.
[14] S. Zhang, A. Garcia-D'Angeli, J.P. Brennan, Q. Huo, Predicting detection limits of enzyme-linked immunosorbent assay (ELISA) and bioanalytical techniques in general, The Analyst. 139 (2014) 439–45. https://doi.org/10.1039/c3an01835k.
[15] S. Ray, G. Mehta, S. Srivastava, Label-free detection techniques for protein microarrays: prospects, merits and challenges, Proteomics. 10 (2010) 731–48. https://doi.org/10.1002/pmic.200900458.
[16] K. Chang, Y. Pi, W. Lu, F. Wang, F. Pan, F. Li, S. Jia, J. Shi, S. Deng, M. Chen, Label-free and high-sensitive detection of human breast cancer cells by aptamer-based leaky surface acoustic wave biosensor array, Biosens. Bioelectron. 60 (2014) 318–24. https://doi.org/10.1016/j.bios.2014.04.027.
[17] M. Espinoza-Castaneda, A. de la Escosura-Muniz, A. Chamorro, C. de Torres, A. Merkoci, Nanochannel array device operating through Prussian blue nanoparticles for sensitive label-free immunodetection of a cancer biomarker, Biosens. Bioelectron. 67 (2015) 107–14. https://doi.org/10.1016/j.bios.2014.07.039.
[18] H.V. Tran, B. Piro, S. Reisberg, L. Huy Nguyen, T. Dung Nguyen, H.T. Duc, M.C. Pham, An electrochemical ELISA-like immunosensor for miRNAs detection based on screen-printed gold electrodes modified with reduced graphene oxide and carbon nanotubes, Biosens. Bioelectron. 62 (2014) 25–30. https://doi.org/10.1016/j.bios.2014.06.014.
[19] A.E. Kennedy, K.S. Sheffield, J.K. Eibl, M.B. Murphy, R. Vohra, J.A. Scott, G.M. Ross, A Surface Plasmon Resonance Spectroscopy Method for Characterizing Small-Molecule Binding to Nerve Growth Factor, J. Biomol. Screen. 21 (2016) 96–100. https://doi.org/10.1177/1087057115607814.
[20] K.S. Sheffield, R. Vohra, J.A. Scott, G.M. Ross, Using surface plasmon resonance spectroscopy to characterize the inhibition of NGF-p75(NTR) and proNGF-p75(NTR) interactions by small molecule inhibitors, Pharmacol. Res. 103 (2016) 292–9. https://doi.org/10.1016/j.phrs.2015.12.005.
[21] K. Mosbach, Molecular imprinting, Trends Biochem. Sci. 19 (1994) 9–14.
[22] K. Haupt, K. Mosbach, Molecularly imprinted polymers and their use in biomimetic sensors, Chem. Rev. 100 (2000) 2495–504.
[23] L. Ye, K. Mosbach, Molecular imprinting: Synthetic materials as substitutes for biological antibodies and receptors, Chem. Mater. 20 (2008) 859–868. https://doi.org/10.1021/cm703190w.
[24] A.G. Ayankojo, A. Tretjakov, J. Reut, R. Boroznjak, A. Öpik, J. Rappich, A. Furchner, K. Hinrichs, V. Syritski, Molecularly Imprinted Polymer Integrated with a Surface Acoustic Wave Technique for Detection of Sulfamethizole, Anal. Chem. 88 (2016) 1476–84. https://doi.org/10.1021/acs.analchem.5b04735.
[25] A. Tretjakov, V. Syritski, J. Reut, R. Boroznjak, O. Volobujeva, A. Öpik, Surface molecularly imprinted polydopamine films for recognition of immunoglobulin G, Microchim. Acta. 180 (2013) 1433–1442. https://doi.org/10.1007/s00604-013-1039-y.
[26] A. Tretjakov, V. Syritski, J. Reut, R. Boroznjak, A. Öpik, Molecularly imprinted polymer film interfaced with Surface Acoustic Wave technology as a sensing platform for label-free protein detection, Anal. Chim. Acta. 902 (2016) 182–188. https://doi.org/10.1016/j.aca.2015.11.004.
[27] P.S. Sharma, A. Pietrzyk-Le, F. D'Souza, W. Kutner, Electrochemically synthesized polymers in molecular imprinting for chemical sensing, Anal. Bioanal. Chem. 402 (2012) 3177–204. https://doi.org/10.1007/s00216-011-5696-6.
[28] P. Jolly, V. Tamboli, R.L. Harniman, P. Estrela, C.J. Allender, J.L. Bowen, Aptamer-MIP hybrid receptor for highly sensitive electrochemical detection of prostate specific antigen, Biosens. Bioelectron. 75 (2016) 188–95. https://doi.org/10.1016/j.bios.2015.08.043.
[29] S. Viswanathan, C. Rani, S. Ribeiro, C. Delerue-Matos, Molecular imprinted nanoelectrodes for ultra sensitive detection of ovarian cancer marker, Biosens. Bioelectron. 33 (2012) 179–183. https://doi.org/10.1016/j.bios.2011.12.049.
[30] Y.T. Wang, Z.Q. Zhang, V. Jain, J.J. Yi, S. Mueller, J. Sokolov, Z.X. Liu, K. Levon, B. Rigas, M.H. Rafailovich, Potentiometric sensors based on surface molecular imprinting: Detection of cancer biomarkers and viruses, Sens. Actuators B-Chem. 146 (2010) 381–

387. https://doi.org/10.1016/j.snb.2010.02.032.
[31] V.V. Shumyantseva, T.V. Bulko, L.V. Sigolaeva, A.V. Kuzikov, A.I. Archakov, Electrosynthesis and binding properties of molecularly imprinted poly-o-phenylenediamine for selective recognition and direct electrochemical detection of myoglobin, Biosens. Bioelectron. 86 (2016) 330–336. https://doi.org/10.1016/j.bios.2016.05.101.
[32] B.V.M. Silva, B.A.G. Rodríguez, G.F. Sales, M.D.P.T. Sotomayor, R.F. Dutra, An ultrasensitive human cardiac troponin T graphene screen-printed electrode based on electropolymerized-molecularly imprinted conducting polymer, Biosens. Bioelectron. 77 (2016) 978–985. https://doi.org/10.1016/j.bios.2015.10.068.
[33] J.L. Urraca, C.S.A. Aureliano, E. Schillinger, H. Esselmann, J. Wiltfang, B. Sellergren, Polymeric Complements to the Alzheimer's Disease Biomarker β-Amyloid Isoforms Aβ1–40 and Aβ1–42 for Blood Serum Analysis under Denaturing Conditions, J. Am. Chem. Soc. 133 (2011) 9220–9223. https://doi.org/10.1021/ja202908z.
[34] A. Cecchini, V. Raffa, F. Canfarotta, G. Signore, S. Piletsky, M.P. MacDonald, A. Cuschieri, In Vivo Recognition of Human Vascular Endothelial Growth Factor by Molecularly Imprinted Polymers, Nano Lett. 17 (2017) 2307–2312. https://doi.org/10.1021/acs.nanolett.6b05052.
[35] Y. Kamon, T. Takeuchi, Molecularly Imprinted Nanocavities Capable of Ligand-Binding Domain and Size/Shape Recognition for Selective Discrimination of Vascular Endothelial Growth Factor Isoforms, ACS Sens. 3 (2018) 580–586. https://doi.org/10.1021/acssensors.7b00622.
[36] M. Johari-Ahar, P. Karami, M. Ghanei, A. Afkhami, H. Bagheri, Development of a molecularly imprinted polymer tailored on disposable screen-printed electrodes for dual detection of EGFR and VEGF using nano-liposomal amplification strategy, Biosens. Bioelectron. 107 (2018) 26–33. https://doi.org/10.1016/j.bios.2018.02.005.
[37] A. Kidakova, J. Reut, R. Boroznjak, A. Öpik, V. Syritski, Advanced sensing materials based on molecularly imprinted polymers towards developing point-of-care diagnostics devices, Proc. Est. Acad. Sci. 68 (2019) 158–167. https://doi.org/10.3176/proc.2019.2.07.
[38] A.P. Davenport, F.D. Russell, Radioligand Binding Assays: Theory and Practice, in: Curr. Dir. Radiopharm. Res. Dev., Stephen J Mather, 1996: pp. 169–178. http://public.ebookcentral.proquest.com/choice/publicfullrecord.aspx?p=3102748.
[39] Y. Gao, X. Li, L.-H. Guo, Development of a label-free competitive ligand binding assay with human serum albumin on a molecularly engineered surface plasmon resonance sensor chip, Anal. Methods. 4 (2012) 3718–3723. https://doi.org/10.1039/C2AY25780G.
[40] A. Kidakova, J. Reut, J. Rappich, A. Öpik, V. Syritski, Preparation of a surface-grafted protein-selective polymer film by combined use of controlled/living radical photopolymerization and microcontact imprinting, React. Funct. Polym. 125 (2018) 47–56.
[41] R.A. Latour, The Langmuir isotherm: A commonly applied but misleading approach for the analysis of protein adsorption behavior, J. Biomed. Mater. Res. A. 103 (2015) 949–958. https://doi.org/10.1002/jbm.a.35235.
[42] R.J. Umpleby, S.C. Baxter, A.M. Rampey, G.T. Rushton, Y.Z. Chen, K.D. Shimizu, Characterization of the heterogeneous binding site affinity distributions in molecularly imprinted polymers, J. Chromatogr. B-Anal. Technol. Biomed. Life Sci. 804 (2004) 141–149.
[43] R.J. Umpleby, S.C. Baxter, M. Bode, J.K. Berch, R.N. Shah, K.D. Shimizu, Application of the Freundlich adsorption isotherm in the characterization of molecularly imprinted polymers, Anal. Chim. Acta. 435 (2001) 35–42.
[44] M. Hellman, U. Arumäe, L. Yu, P. Lindholm, J. Peränen, M. Saarma, P. Permi, Mesencephalic astrocyte-derived neurotrophic factor (MANF) has a unique mechanism to rescue apoptotic neurons, J. Biol. Chem. 286 (2011) 2675–2680. https://doi.org/10.1074/jbc.M110.146738.
[45] V. Parkash, P. Lindholm, J. Peränen, N. Kalkkinen, E. Oksanen, M. Saarma, V.-M. Leppänen, A. Goldman, The structure of the conserved neurotrophic factors MANF and CDNF explains why they are bifunctional, Protein Eng. Des. Sel. 22 (2009) 233–241. https://doi.org/10.1093/protein/gzn080.

[46] E. Galli, A. Planken, L. Kadastik-Eerme, M. Saarma, P. Taba, P. Lindholm, Increased Serum Levels of Mesencephalic Astrocyte-Derived Neurotrophic Factor in Subjects With Parkinson's Disease, Front. Neurosci. 13 (2019). https://doi.org/10.3389/fnins.2019.00929.

Figures

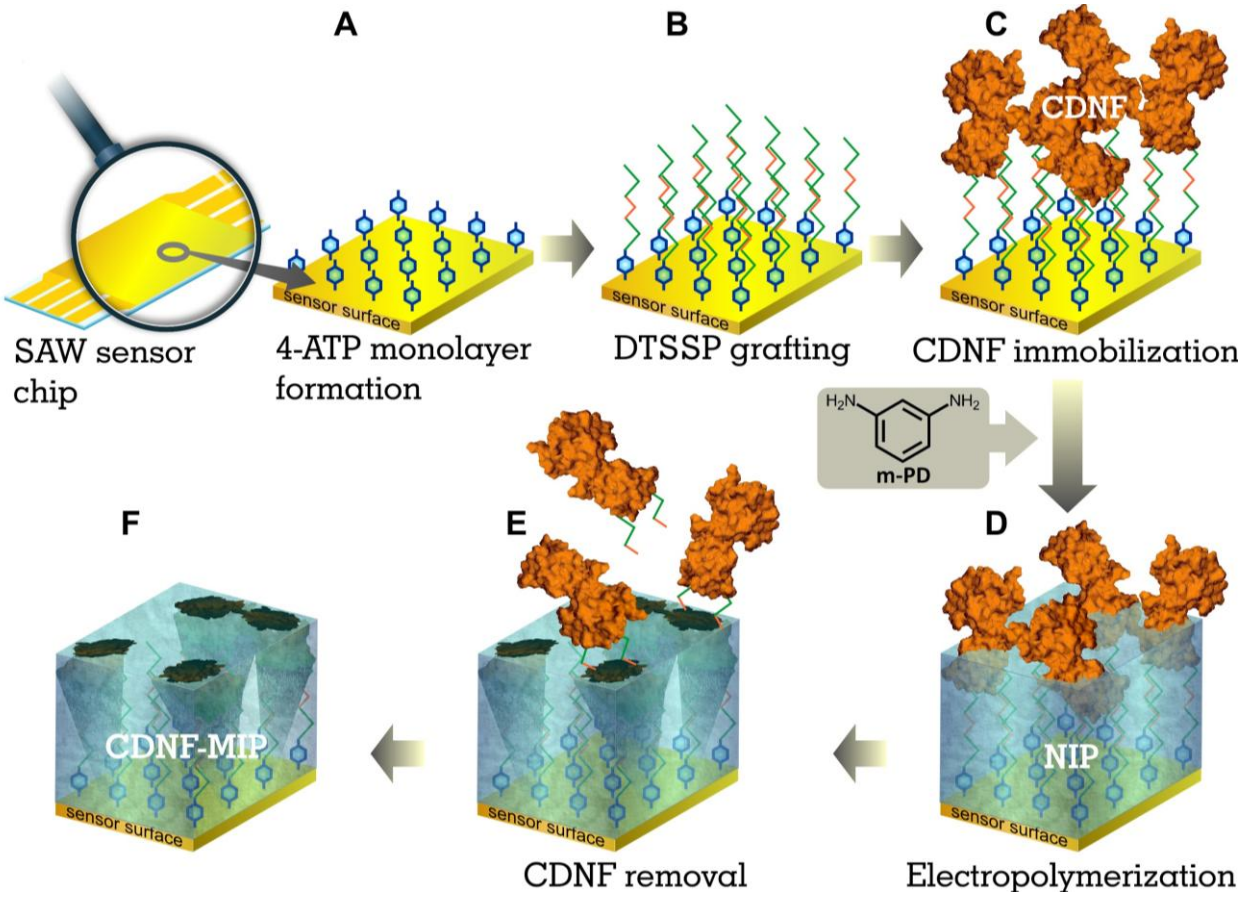

Figure 1. The surface imprinting strategy for synthesis of the CDNF-MIP layer on the gold sensing surface of the SAW chip using the electropolymerization approach.

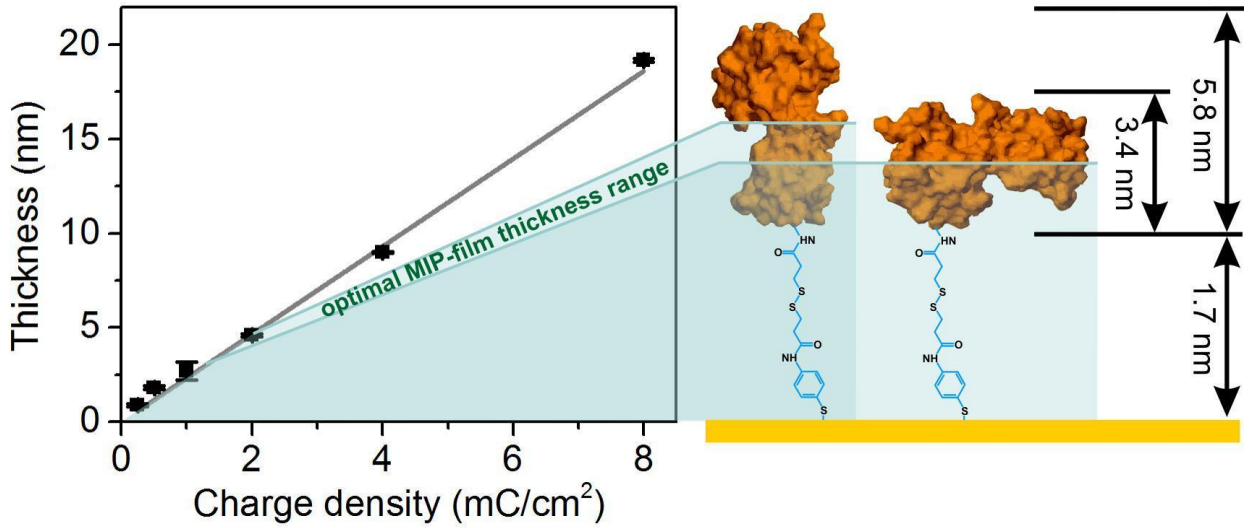

Figure 2. The calibration graph representing the dependence of the polymeric thickness of MIP films, as measured by VIS-ellipsometry, on the amount of the charge consumed during the electropolymerization of *m*-PD on CDNF-modified gold electrode. The solid lines represent linear regression fits. The drawing on the right hand of the figure demonstrates an approximation of the heights of the linker-CDNF structure immobilized on a planar surface.

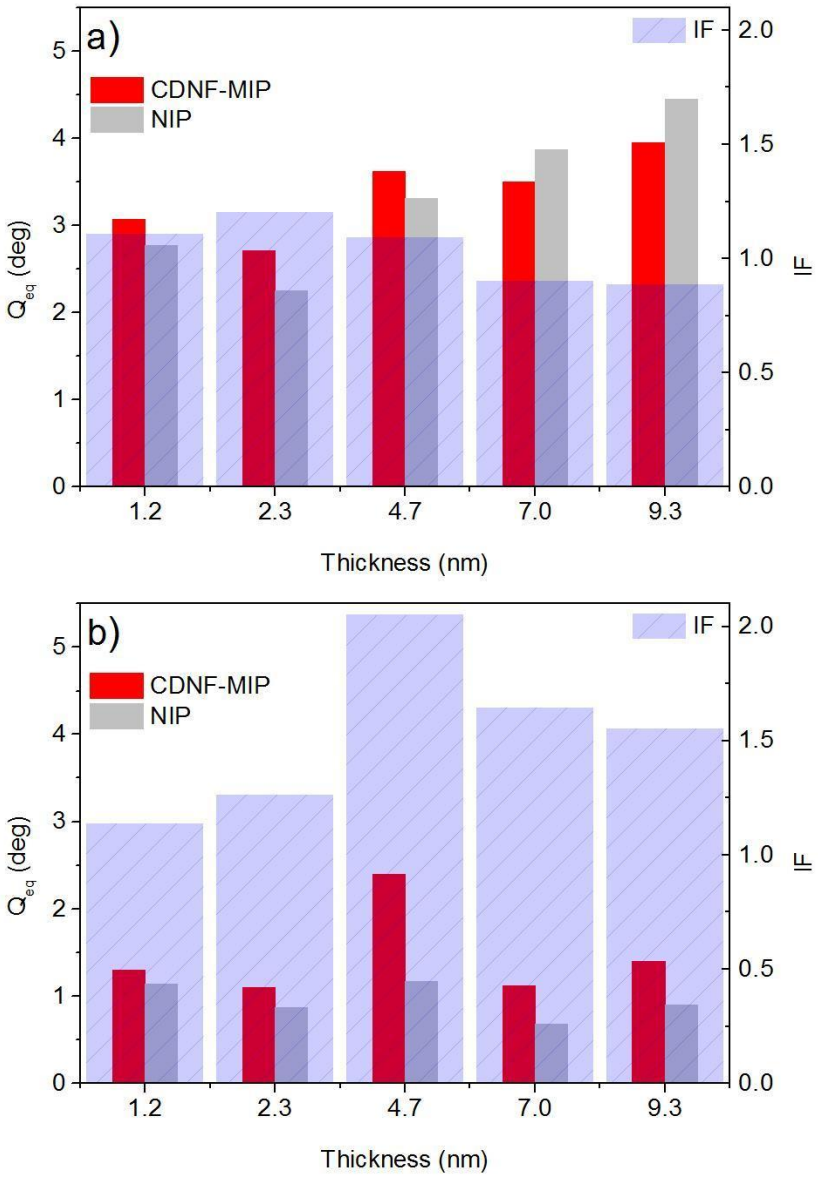

Figure 3. Effect of the polymer thickness of CDNF-MIP and NIP films on the responses of the SAW sensors and the respective imprinting factors measured upon injection of 1.25 µg/mL of CDNF in PBS: a) without blocking of nonspecific adsorption b) after blocking in 0.1 M PBS buffer (pH 7.4) containing 0.04 mg/ml HSA.

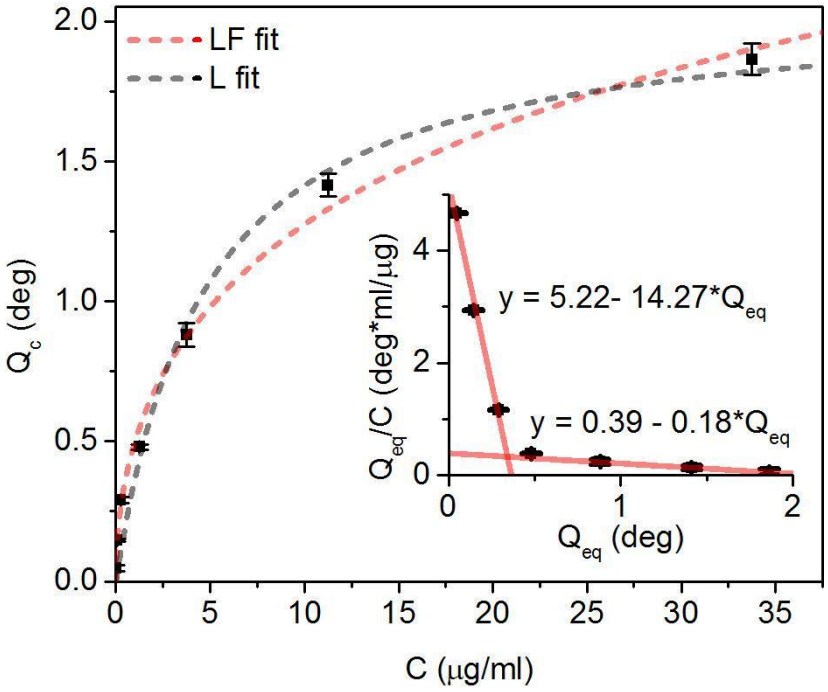

Figure 4. The adsorption isotherm of CDNF measured by CDNF-MIP sensor. The dashed lines represent fits to the Langmuir (gray) and Langmuir-Freundlich (red) adsorption models. Insert: the Scatchard plot with limiting slopes estimates by means of linear regression.

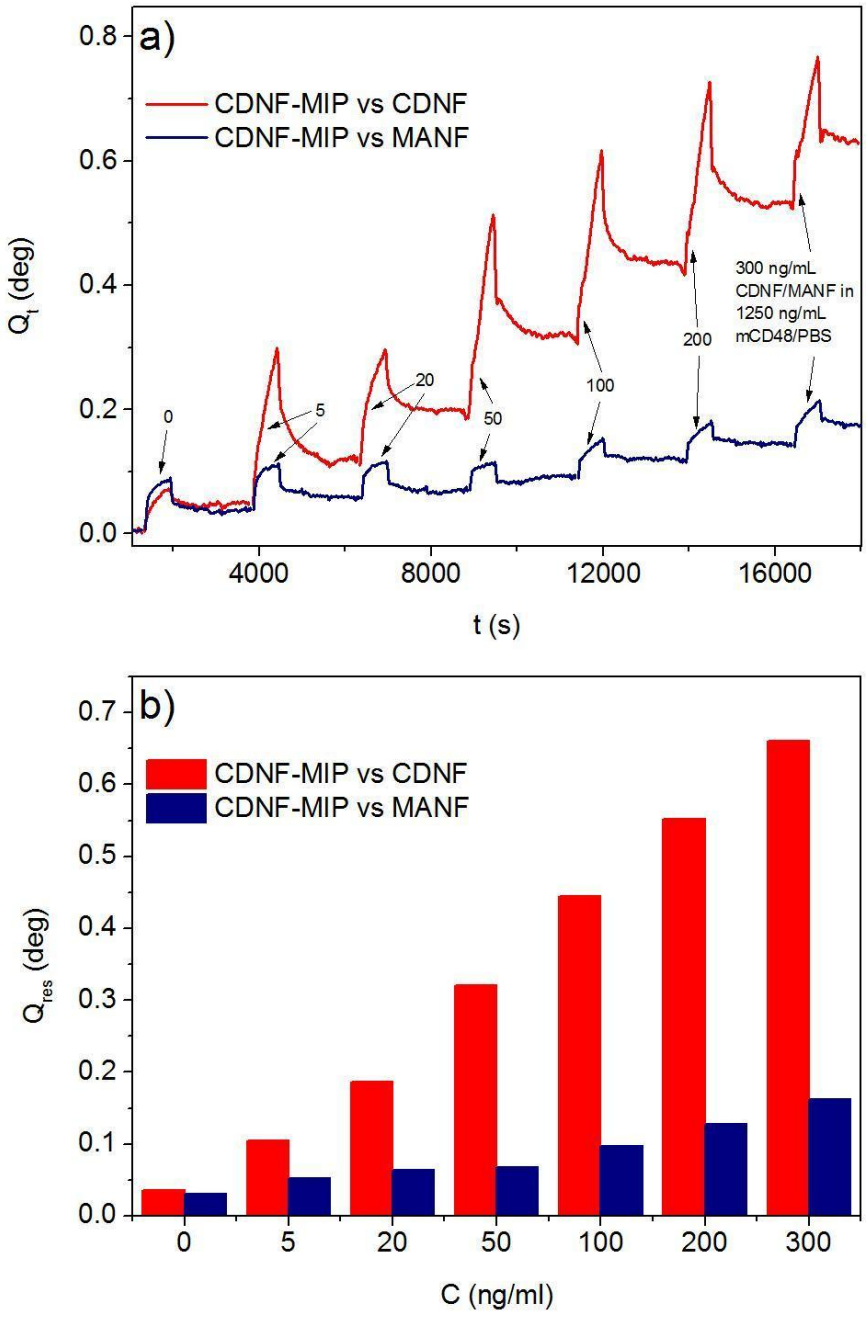

Figure 5. (a) The NIP-corrected sensorgrams of CDNF-MIP sensor measured by the kinetic titration method upon injections of different concentrations of CDNF (red) or MANF (blue) in the presence of 1.25 µg/ml mCD48 and (b) the corresponding residual responses at infinite dissociation derived from Eq. S4 (see section S2).

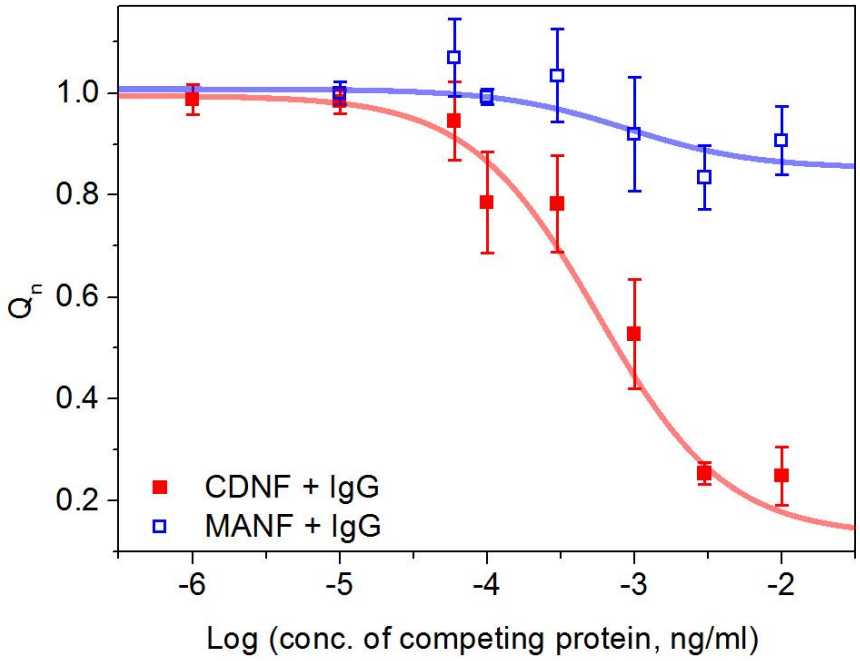

Figure 6. Competitive binding of IgG measured by CDNF-MIP sensor as a function of the competing protein concentration (ng/ml). The binding was conducted in PBS buffer solution containing a fixed concentration of IgG (500 ng/ml) and increasing concentration of the competing protein, either CDNF or MANF, in the range of 10^{-6} to 10^{-2} ng/ml. The sensor responses were normalized to the response upon injection of IgG (500 ng/ml).

Highlights

- CDNF-MIP was reliably interfaced with a SAW sensing platform by electropolymerization of m-phenylenediamine.
- The influence of polymer matrix thickness in CDNF-MIP on the effect of imprinting was studied.
- The CDNF-MIP sensor was able to recognize CDNF in the presence of interfering proteins in the range of sub pg/ml.

Figure 1

Click here to download high resolution image

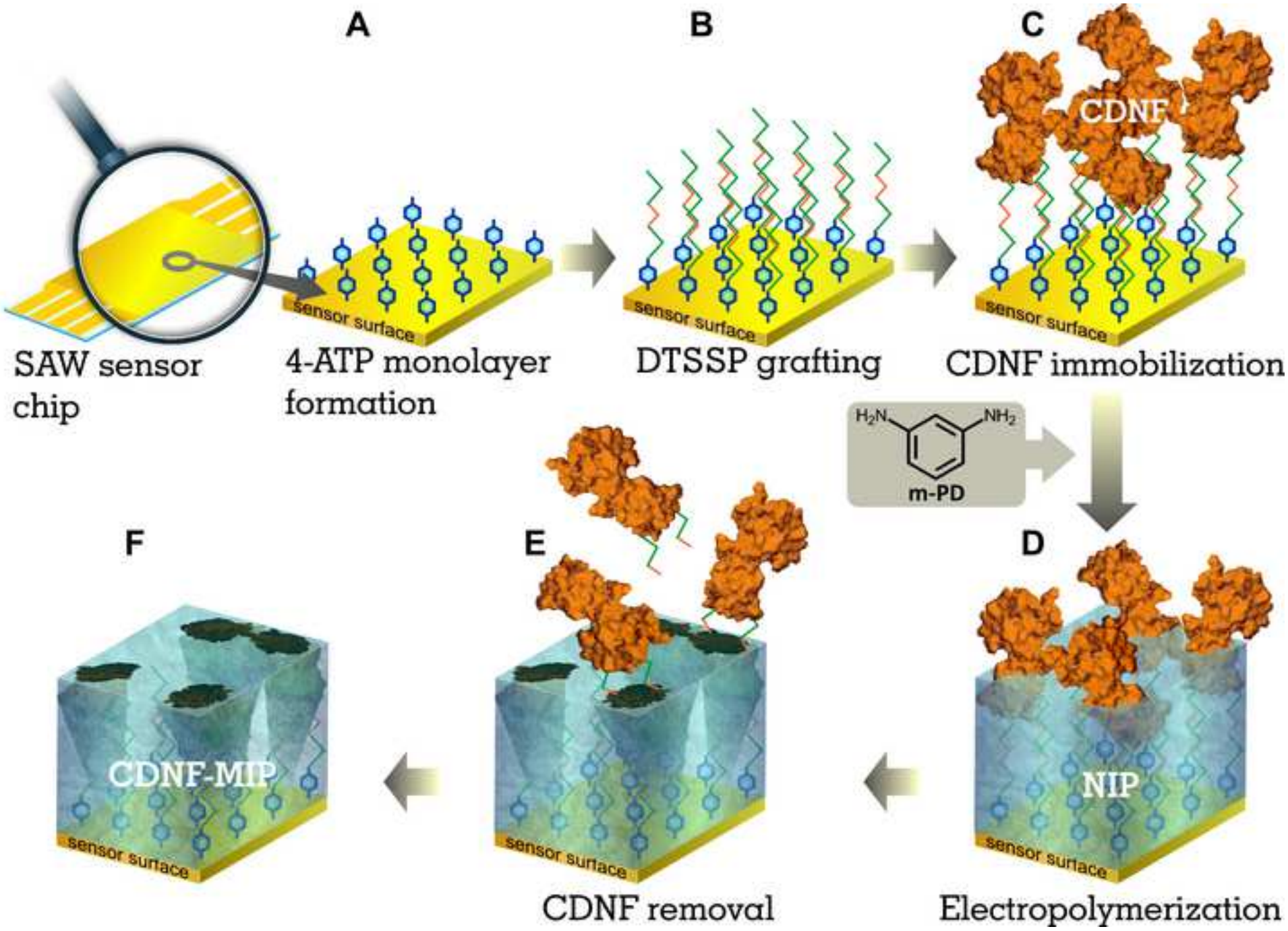

Figure 2

Click here to download high resolution image

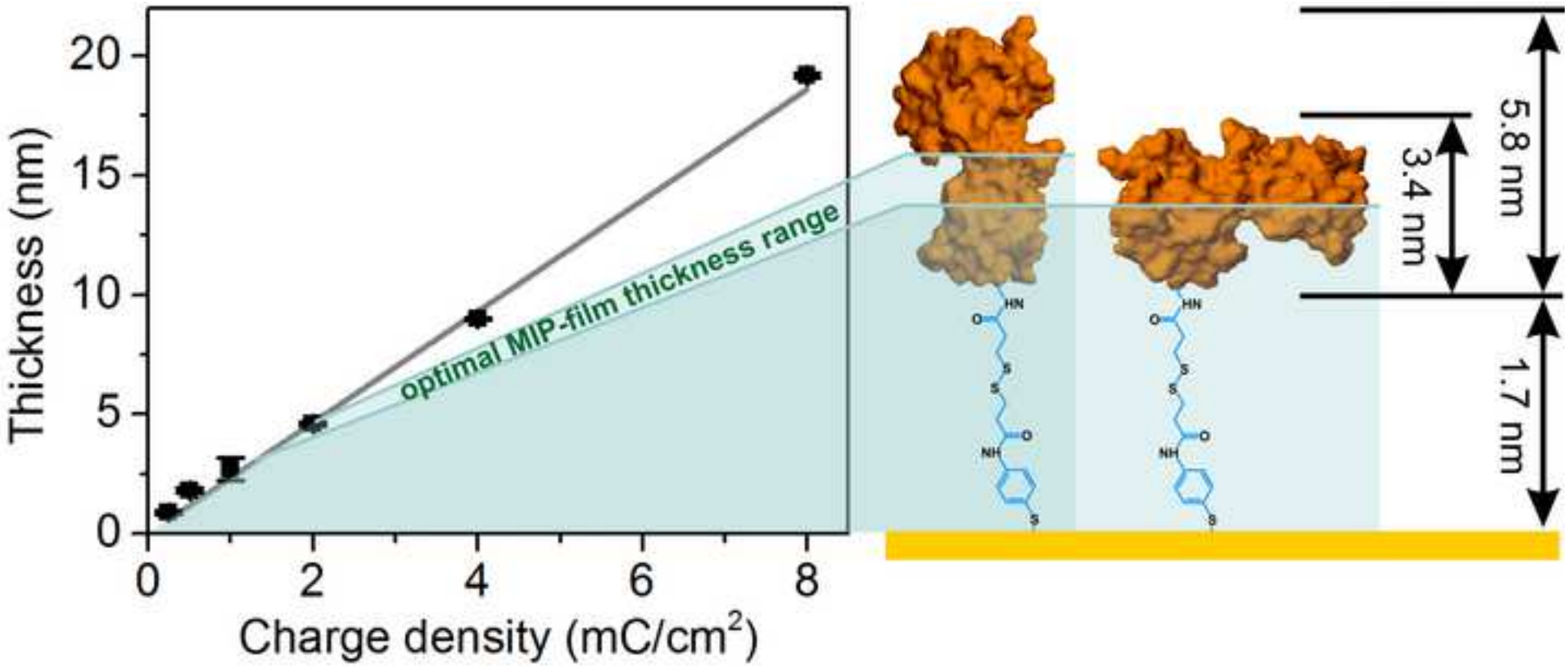

Figure 3

Click here to download high resolution image

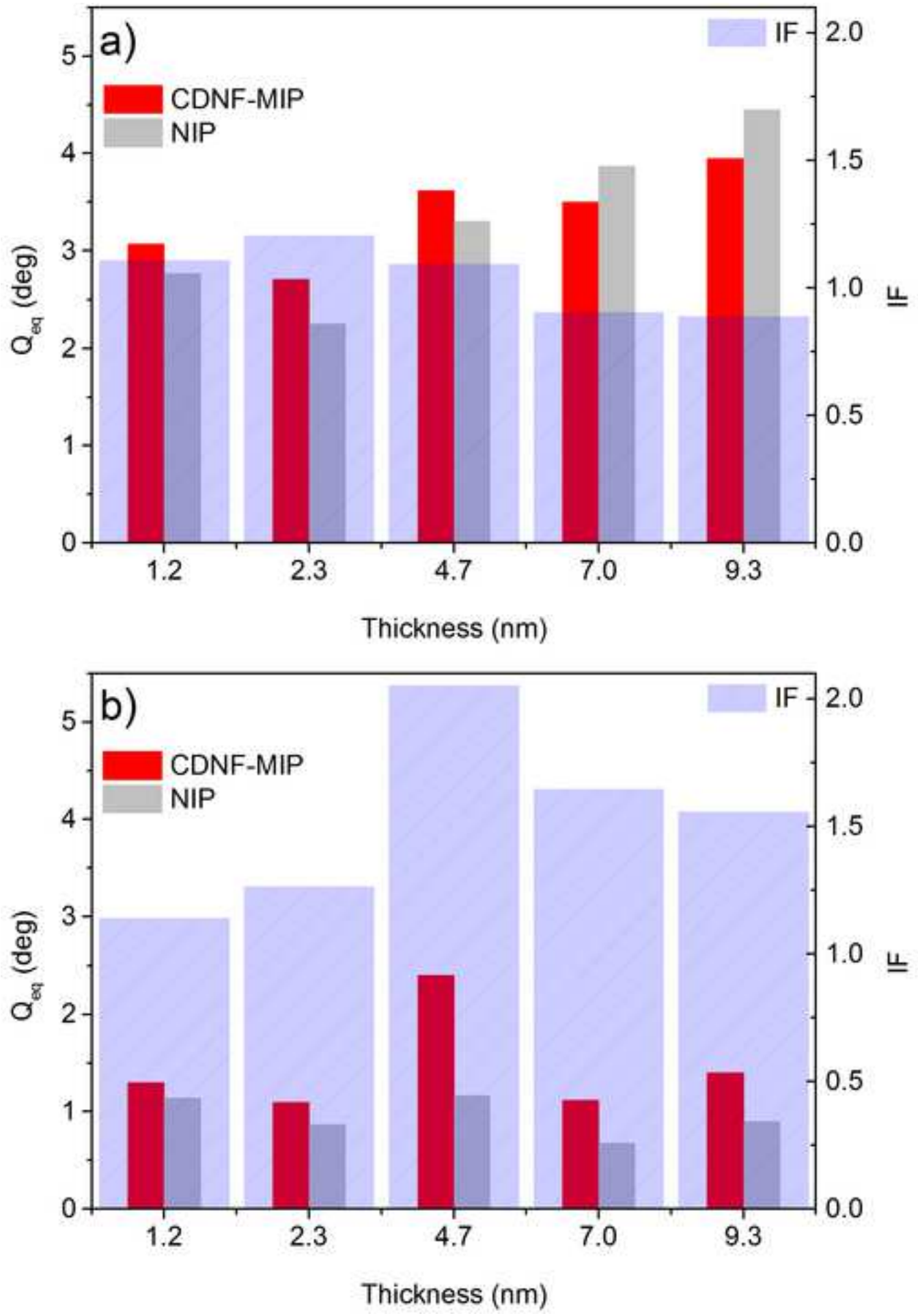

Figure 4

Click here to download high resolution image

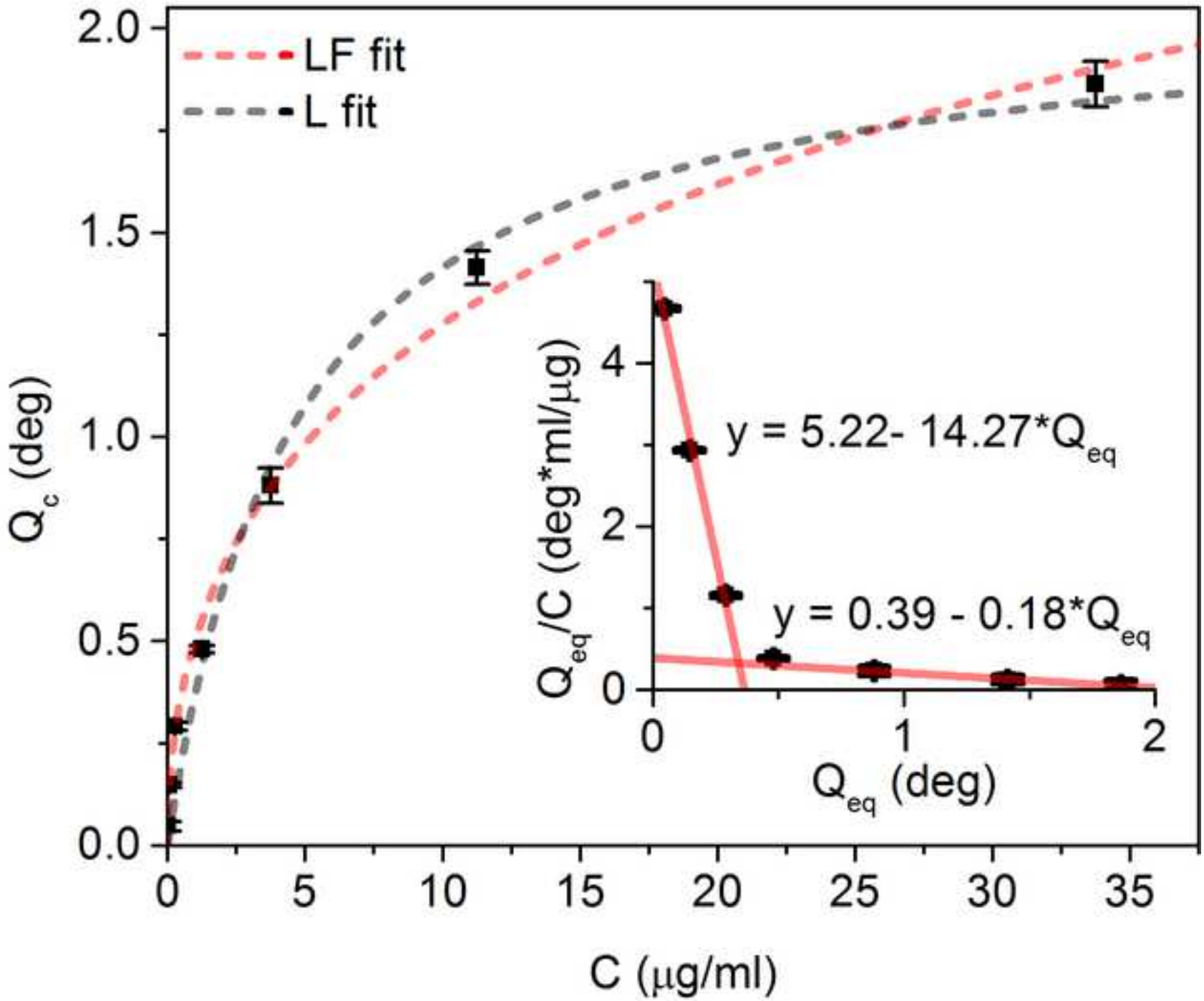

Figure 5

Click here to download high resolution image

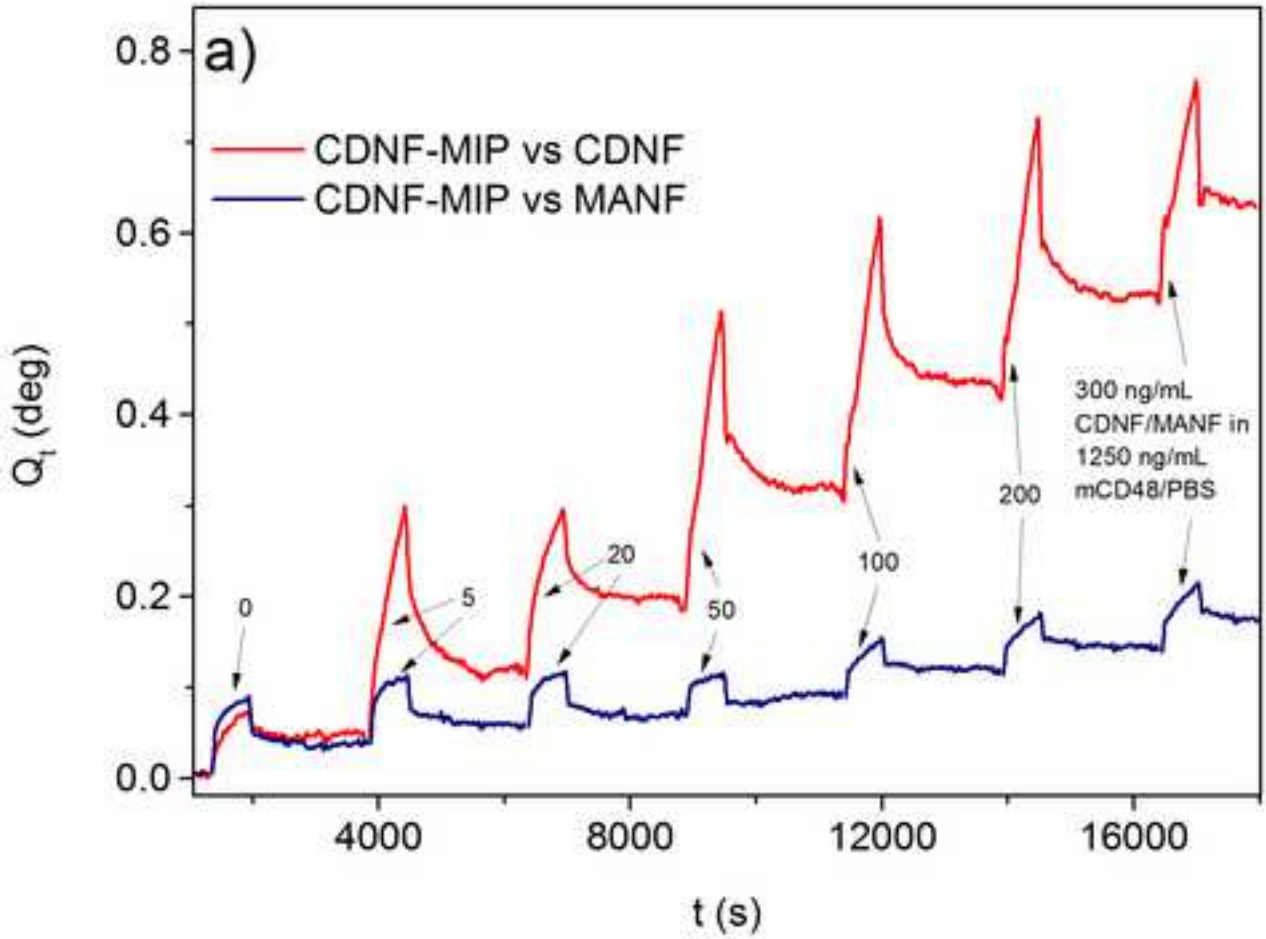

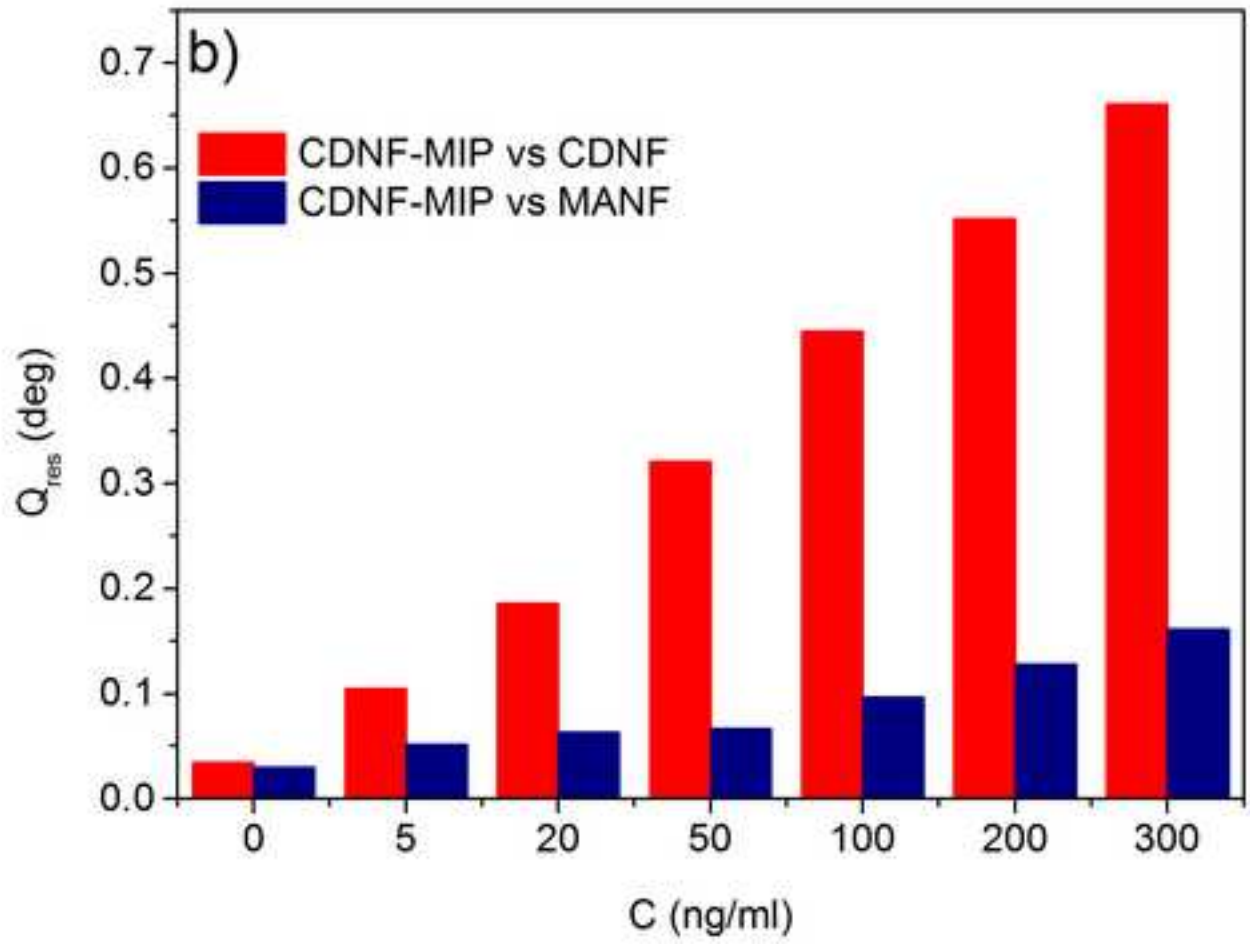

Figure 6

Click here to download high resolution image

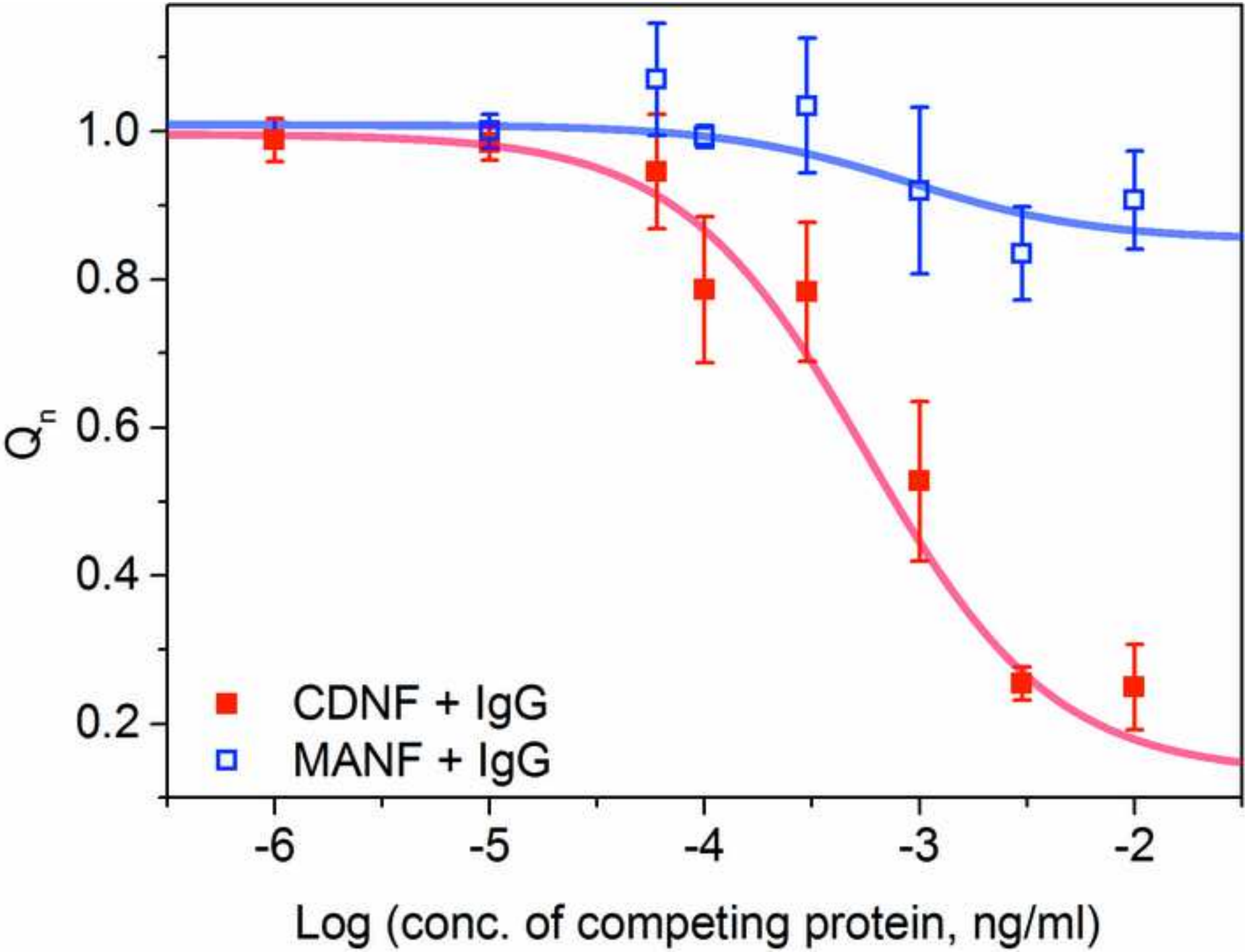

Supplementary Material

Click here to download Supplementary Material: SI-cdnf-mip (R02).pdf

***Author Biographies**

Anna Kidakova graduated from Astrakhan State Technical University in 2007. She received her MSc (2014) in material sciences from TalTech. She is currently a PhD student at the Laboratory of Biofunctional Materials of TalTech. Her research interest includes the development of molecularly imprinted polymer-based sensors for point-of care application.

Roman Borozнjak received his MSc (2007) in organic chemistry and PhD (2017) in natural and exact sciences from TalTech. His research interests include computational modelling and rational design of molecularly imprinted polymers.

Jekaterina Reut is currently a research scientist at the Department of Material and Environmental Technology in TalTech. She received her PhD (2004) in the field of electrically conducting polymers from TalTech. Her research interest is in the area of the design and synthesis of molecularly imprinted polymers for biosensing applications.

Andres Öpik received his PhD in chemistry from the University of Tartu in 1980. He is currently Professor of physical chemistry at the Department of Material and Environmental Technology in TalTech. His main research field is material science and technology: investigation of the physical and chemical properties and possibilities of practical applications of different electronic materials such as electrically conductive polymers and inorganic semiconductive compounds. Currently his research interests include the development of novel functional materials based on molecularly imprinted polymers for biomedical diagnostics.

Mart Saarma received his PhD in 1975 in Molecular Biology at the University of Tartu. Currently he is the head of the Laboratory of Molecular Neuroscience at the Institute of Biotechnology, HiLIFE, University of Helsinki. He is investigating the structure, biology and therapeutic potential of neurotrophic factors. His group has characterized several new GDNF family receptors and novel neurotrophic factor CDNF that is in Phase I-II clinical trials on Parkinson's disease patients.

Vitali Syritski received his PhD in Chemistry at Tallinn University of Technology in 2004. Currently he is the head of the Laboratory of Biofunctional Materials in the Department of Material and Environmental Technology at TalTech. His present research interests include molecularly imprinted technology and electrochemical analysis. In particular, he has focused on development of chemical and biosensors for accurate and fast detection of disease biomarkers and environmental contaminants.

***Declaration of Interest Statement**

Declaration of interests

☒ The authors declare that they have no known competing financial interests or personal relationships that could have appeared to influence the work reported in this paper.

☐The authors declare the following financial interests/personal relationships which may be considered as potential competing interests: